CHEMISTRY
A EUROPEAN JOURNAL

DOI: 10.1002/chem.200500047

Spectroscopic Studies of Water-Soluble Porphyrins with Protein Encapsulated in Bis(2-ethylhexyl)sulfosuccinate (AOT) Reverse Micelles: Aggregation versus Complexation

Suzana M. Andrade* and Sílvia M. B. Costa[a]

Abstract: We have investigated the interaction of two water-soluble free-base porphyrins (negatively charged *meso*-tetrakis(*p*-sulfonatophenyl)porphyrin sodium salt (TSPP) and positively charged *meso*-tetrakis(*N*-methylpyridinium-4-yl)porphyrin (TMpyP)) with two drug-carrier proteins (human serum albumin (HSA) and β-lactoglobulin (βLG)) in bis(2-ethylhexyl)sulfosuccinate (AOT)/isooctane/water reverse micelles (RM) by using steady-state and transient-state fluorescence spectroscopy. TSPP exhibited a complex pattern of aggregation on varying the RM size and pH in the absence of the protein: at low ω_0 (the ratio of water concentration to AOT concentration, the emission of H-aggregates prevails under acidic or neutral "pH_{ext}" conditions. Upon formation of the water-pool, J-aggregates and monomeric diacid species dominate at low "pH_{ext}" but only monomer is detected at neutral "pH_{ext}". The aggregation number increases with ω_0 and the presence of the protein does not seem to contribute to further growth of the aggregate. The presence of protein leads to H-deaggregation but promotes J-aggregation up to a certain protein/porphyrin ratio above which, complexation with the monomer bound to a hydrophobic site of the protein prevails. The effective complex binding constants are smaller than in free aqueous solution; this indicates a weaker binding in these RM probably due to some conformational changes imposed by encapsulation. Only a weak quenching of TMpyP fluorescence is detected due to the presence of protein in contrast to the negative porphyrin.

Keywords: aggregation · binding · porphyrinoids · proteins · reverse micelles

Introduction

There has been a growing interest in the use of porphyrins and related compounds as therapeutic drugs in important areas such as cancer detection, as photosensitizers in photodynamic therapy,[1] or as catalysts in oxidation processes.[2] Biological effects of porphyrins largely depend on their physicochemical properties and may involve mechanisms of membrane penetration or plasma–protein binding.[3] However, porphyrins are usually introduced into the blood as relatively concentrated solutions the activity of which may diminish, or that may cause adverse effects due to spontaneous aggregation processes.[4] In this context, water-soluble porphyrins are interesting because their self-aggregation can lead to defined ordered structures if the selective noncovalent interactions are carefully controlled.[5] A variety of such self-assembled organizates gives a structure that can be classified as J- and H-type aggregates corresponding to the limiting cases of parallel monomeric units stacked edge-to-edge or face-to-face, respectively. In particular, the anionic porphyrin *meso*-tetrakis(*p*-sulfonatophenyl)porphyrin sodium salt (TSPP) was reported to self-aggregate under certain conditions of concentration, low pH, and/or high ionic strength.[6] The structure consists of in-line homoassociated arrays and it is stabilized through a hydrogen bond network acting between the anionic sulfonate groups and the charged protonated nitrogen atoms.[7]

The size and shape of the J-aggregate structures have been estimated from light scattering experiments (small-angle X-ray scattering (SAXS);[8] dynamic light scattering (DLS);[9] resonance light scattering (RLS)[10]). Evidence for rod-like aggregates with $\sim 10^4$ molecules along the principal axis and 20 molecules across the diameter was given along with a structure described in terms of fractal geometry.[11]

[a] Dr. S. M. Andrade, Prof. Dr. S. M. B. Costa
Centro de Química Estrutural, Complexo 1
Instituto Superior Técnico, 1049–001 Lisboa (Portugal)
Fax: (+351) 21-846-4455
E-mail: sandrade@mail.ist.utl.pt

Supporting information for this article is available on the WWW under http://www.chemeurj.org/ or from the author.

AFM images of TSPP J-aggregates coated on silicon substrates also showed that stripe-like clusters located on the surface have lengths similar to those estimated by DLS.[12] The aggregation numbers (N) compare relatively well with those reported using spectroscopic techniques $N=11$–26.[6a,13] The kinetics of the aggregation process can also be deduced by using absorption spectroscopy that can differentiate clearly between monomeric and aggregated species.[14]

Recently, it was reported that these aggregates could be promoted in the presence of template agents such as surfactants,[13,15] proteins,[16] and dendrimers.[17] In the present study, we aimed to extend our earlier work on protein–porphyrin complexation and induced self-aggregation of porphyrins in aqueous solution (see Results) to reverse micelles, that represent a useful alternative microheterogeneous medium.

Reverse micelles (RM) are stable dispersions of water in nonpolar solvents and have been used extensively as biological membrane models to aid in the understanding of membrane chemistry.[18] By far, the most common system used in RM studies is the ternary mixture consisting of the anionic surfactant sodium bis(2-ethylhexyl)sulfosuccinate (AOT)/nonpolar-solvent/water, formed at concentrations above 1 mM.[19] These RM have the ability to solubilize large amounts of water and form spherical monodisperse droplets that do not vary with dispersed-phase volume fraction and temperature.[20] The entrapped water influences RM radius, shape, and polar headgroup packing.[21] Therefore, the parameter ω_0, $\omega_0=$[water]/[AOT], has been used to describe these systems and was shown to be directly proportional to the micellar radius.[19a] FTIR and NMR spectroscopy indicate that water molecules solubilized inside small micelles ($\omega_0 \leq 7$) are in contact with and bound to the polar headgroups of AOT, thus inhibiting their ability to form hydrogen bonds as found in bulk water.[22] Solvation dynamics also showed that water inside the smallest micelles is immobilized, but a bulk-like component appears as water is added and a water core forms.[23]

The role of water-in-oil (w/o), RM, or microemulsions as nanoreactors and the interactions with several water-soluble porphyrins and cyanines was explored[15b,24] and could be a means to control the size of nanoparticles. In this context, we studied the role of spatial confinement and size of the AOT RM on the aggregation pattern of TSPP and on TSPP–protein interaction at two different pH conditions, at porphyrin concentrations where aggregation in water does not occur. We discuss the complex spectroscopic variation found upon changing the water amount in terms of J- and H-type aggregates and correlate this with time-resolved fluorescence data. Data are further compared with that obtained with the positively charged *meso*-tetrakis(*N*-methylpyridinium-4-yl)porphyrin (TMpyP). In contrast to TSPP, we do not detect aggregation of the TMpyP porphyrin either by the protein or encapsulation in AOT RM.

Results

TSPP–protein interaction in aqueous solution

We have shown in previous studies that drug-carrier proteins such as HSA (submicromolar amounts) and βLG (micromolar amounts) could act as templates for the formation of TSPP J-aggregates in acidic solutions (pH 2, where TSPP has a zwitterionic nature (I), see Scheme 1), but not under

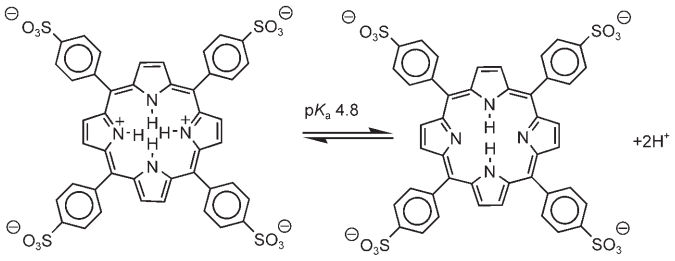

Scheme 1. Acid–base equilibrium of TSPP in aqueous solution.

neutral pH conditions (tetraanionic free-base porphyrin (II), see Scheme 1).[16b] These were characterized spectroscopically by the appearance of two new absorption bands (see Table 1) at 490 nm (B-band) and at 705 nm (Q-band), as well as by the induction of a circular dichroism (CD) signal at those wavelengths, and a dependence on the excitation and emission wavelengths. Increasing amounts of both proteins leads to a new spectroscopic pattern attributed to the formation of a complex porphyrin–protein with relatively high binding constants, $K_B \sim 3$–$5\times10^6\,M^{-1}$ and where electrostatic interactions prevail. The interaction with HSA resulted in a Soret band at 420 nm independent of solution pH, that is, blue-shifted compared with the diprotonated monomer (from 434 to 420 nm) and red-shifted compared with the free-base TSPP (from 413 to 420 nm), whereas in the presence of βLG the peak shifts (~3 nm) to lower energy relative to the free-base TSPP. Fluorescence quenching of Trp residues of these proteins indicated different locations for TSPP and suggested a mechanism of efficient energy transfer from Trp amino acids to the porphyrin. The type of energy transfer may be derived from the value of R_0, that is, the critical distance at which energy transfer to the acceptor and spontaneous decay of the excited donor are equally probable.[25] The value obtained, $R_0 \sim 56$ Å, suggests a long-distance Forster-type resonance energy transfer (FRET) and stresses the importance of FRET as a tool to determine the spatial distribution of interacting molecules.

TSPP in AOT reverse micelles at variable water content, ω_0

"pH_{ext}" = 2: Solubilization of TSPP in AOT reverse micelles in the absence of water was not possible. At very low ω_0, $\omega_0=3$, a substantial blue-shift was detected for the Soret

Table 1. Absorption and fluorescence emission maxima [nm] of TSPP (1 μM) in some of the studied systems together with data from the literature.

	ω_0	Absorption maxima							Emission maxima	
		Soret	J-agg	Q_y		Q_x		J-agg		
	3–6	402	493[b]	518	555	594	653	703[b]	660	723
	7–9	405 (415)[a]	491.5	–	–	–	–	705	658	716.5
$pH_{ext}=2$	10	420	491	–	–	–	–	705	657	713
	20–50	423.5	490	–	–	–	–	706	672 (718)[c]	716
	water	433.5	–	–	–	593	644	–	674	–
	3–10	405	–	520	557.5	591.5	651.5	–	658	721
	15	408	–	520	558	590	649.5	–	658	718.5
$pH_{ext}=7$	15+HSA	420 (405)[a]	–	519	553.5	591.5	649	–	653.5	719.5
	40	412.5	–	519	556	582.5	646	–	655	710
	water	412.5	–	515.5	552.5	579	633	–	648	708
DMSO[d]		419	–	514.5	550	591	645.5	–	652	718
HSA, R = 0.1[e]		420	489	515	550	591	648	704	655	718
TTAB[f]		416.5	490	512	546	587	642	705	652	719
Triton X-100[g]		417.5	–	513	548	588	644	–	651	717
PAMAM[h]		408	–	521.5	558	595.5	651.5	–	667	728

[a] Shoulder. [b] For $\omega_0=5$. [c] $\lambda_{exc}=495$ nm. [d] [TSPP] = 4 μM. [e] R = [HSA]/[TSPP]. [f] TTAB/heptane–chloroform $\omega_0=15$, "pH_{ext}" = 2. [g] Triton X-100/cyclohexane–hexanol/water, $\omega_0=16$, "pH_{ext}" = 2. [h] PAMAM dendrimers generation 4, [dendrimer]/[porphyrin] = 0.075, "pH_{ext}" = 7.[17a]

band to 402 nm compared with free aqueous solution, Figure 1A.

The deconvolution of the Soret band using a sum of Gaussian functions shows the contribution of two bands with maxima at 405 and 419 nm. The latter resembles that obtained for TSPP in DMSO indicating the existence of porphyrin monomers in a hydrophobic environment, most likely the AOT RM interfacial region. As the amount of water increases, a new band at around 490 nm appears that increases monotonically. This is followed by a concomitant red-shift of the Soret band that at the highest water content studied ($\omega_0=50$) approaches that found for the absorption in water, which suggests that the probe is located near the water pools. Nevertheless, the Soret band shows a much broader band with two maxima at ~420 and 434 nm, that together with an ill-defined isosbestic point, indicates the existence of multiple species.

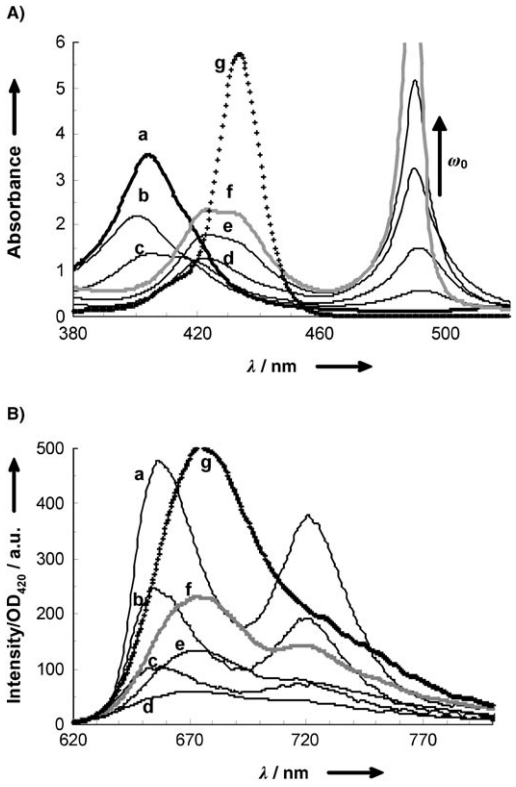

Figure 1. A) Absorption and B) fluorescence emission spectra of TSPP (~1 μM) encapsulated in AOT RM at different ω_0: a) 3; b) 5; c) 9; d) 20; e) 30; f) 40; and g) in free aqueous solution (multiplied by 0.6); pH 2; [AOT] = 0.1 M; $\lambda_{exc}=420$ nm; optical density values are multiplied by 10.

We see significant changes in the fluorescence emission spectra at the different ω_0 values studied, Figure 1B. At low water content ($\omega_0<10$), TSPP fluorescence spectra ($\lambda_{exc}=$ 420 nm) show two well-defined vibronic bands, similar to those found in organic solvents.

Since TSPP is insoluble in AOT/isooctane at the concentration used, the spectra should reveal information about the aqueous interior of the RM but the bands were red-shifted comparatively to free aqueous solution. As the water was increased up to $\omega_0=10$ an important fluorescence quenching occurred (~80%), see Figure 2A, with a small plateau between $\omega_0=6$–7 that corresponds to the appearance of free water molecules. At higher water contents, global fluorescence quantum yields increased again (~65%), but to values (ϕ_f~0.05) below that obtained in acidic aqueous solution ($\phi_f^{H_2O}$~0.14). This was followed by changes in the emission spectra which became less-structured with the main band appearing at ~672 nm at $\omega_0=50$ (approaching the value obtained in water).

Emission spectra were not dependent on excitation wavelength (420 or 495 nm) up to $\omega_0=10$. As we increased the ω_0 value a prominent wavelength-dependent band centered at 718 nm developed that we might attribute to TSPP J-aggregates. Excitation spectra data (not shown) indicated that

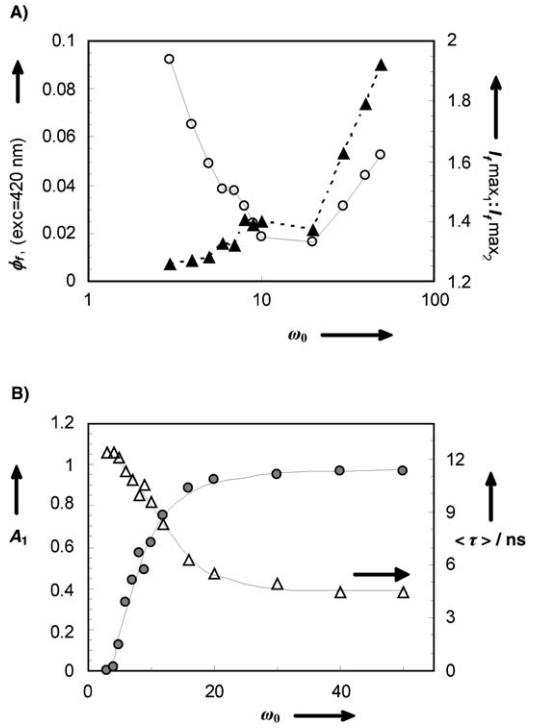

Figure 2. A) Global fluorescence quantum yield of TSPP encapsulated in AOT RM (○) and fluorescence intensity ratio of the two band maxima (▲) at different ω_0; B) Preexponentials associated to the shorter component of TSPP fluorescence lifetimes A_1 (●) and fluorescence mean lifetime, $\langle\tau\rangle$ (Δ) obtained by global analysis fitting. $\lambda_{exc}=420$ nm and $\lambda_{em}=650$ nm; (pH 2; [AOT] = 0.1 M).

fluorescence emission at both 640 and 720 nm at $\omega_0=10$ comes almost exclusively from the monomeric species in the less-hydrophilic region.

Fluorescence lifetimes were obtained upon excitation at 420 nm and read at 650 nm. Under these conditions the decays could only be analyzed by using a sum of two exponentials. We attempted global fitting and determined two quite distinct lifetimes: $\tau_1=3.58$ ns and $\tau_2=12.54$ ns, Figure 2B.

Under similar experimental conditions, a single exponential of $\tau=3.83$ ns[16b] was obtained for TSPP in aqueous acidic solution. The lifetime associated with J-aggregates was reported to be in the picosecond range (50 ps)[13] and lies outside our equipment detection range. The shorter component can be assigned to the monomer in acidic medium; the contribution increases with ω_0 in agreement with the spectroscopic data presented. The long lifetime has already been obtained for TSPP in solvents such as DMSO[16b] when interacting with human serum albumin, in Triton X-100 surfactant aqueous micelles,[13] and in the presence of PAMAM higher-generation dendrimers.[17b] A common interpretation of this lifetime was given suggesting a more hydrophobic environment for TSPP.

"pH_{ext}" = 7: The global charge on the TSPP changes from a dianion at pH 2 to a tetraanion at pH 7 ($pK_a^{water}\approx 4.8$). At this pH, the TSPP absorption spectrum showed the common characteristics of other free-base porphyrins, exhibiting features of D_{2h} symmetry, with the Soret band centered at 413 nm and four quasiallowed Q-bands. By contrast with the single-band emission spectrum obtained in acidic medium, we found two well-defined emission bands with maxima 648 and 708 nm, see Table 1.

The incorporation of TSPP in AOT reverse micelles was only achieved at $\omega_0=3$ (the hydrodynamic radius of the AOT RM is approximately twice that of the porphyrin) and at the lower ω_0 ($\omega_0<7$) the absorption and emission spectra resemble those obtained at $pH_{ext}=2$, that is, no longer dependent on pH, Figure 3A.

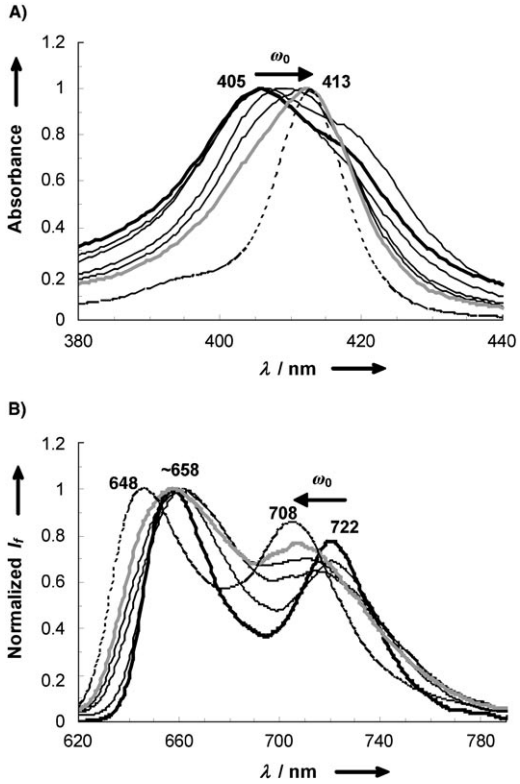

Figure 3. A) Absorption and B) fluorescence spectra of TSPP encapsulated in AOT RM at different water content, $\omega_0=3$ (bold black); $\omega_0=40$ (bold grey), and water (dotted line); pH 7, [TSPP] = 1 μM; $\lambda_{exc}=425$ nm).

The increase in water content led to an increase in absorbance in the Soret band region followed by a concomitant red-shift and band narrowing. At the highest studied ω_0, $\omega_0=40$, the spectrum showed a similar Soret maximum around 412 nm although with a broader band (fwhm ~ 1250 cm^{-1}) than in aqueous solution (fwhm ~850 cm^{-1}).

Furthermore, the absence of an isosbestic point indicated the presence of more than two species in the micellar system, and possibly a distribution. The fluorescence obtained upon excitation at 425 nm, Figure 3B, shows two well-defined bands whose intensity gradually increases as

they shift to the blue with peaks changing from ~658 and 722 nm to 655 and 710 nm, respectively, still red-shifted relatively to those obtained in free water.

The fluorescence decay of the monomer in aqueous solution at pH 7 is monoexponential with $\tau_f = 9.80$ ns ($\lambda_{exc} =$ 420 nm and $\lambda_{em} = 650$ nm).[16b] Higher values were reported in nonbuffered solutions (10.3 ns),[17b] as well as lower values (9.3 ns)[13] but at higher concentrations of the porphyrin (10–50 μM). The decay curves obtained for TSPP in this study upon encapsulation at all studied ω_0 were fitted globally: a major component with a decay time of 12.8 ns (τ_1) similar to that already obtained at pH 2, and another with 7.93 ns (τ_2) were found. The pre-exponential factor a_i, that gives the population of fluorophores with the correspondent lifetime τ_i, indicates that major changes occur at $\omega_0 \leq 10$, where a_1 drops from ~97 to ~50% with the reciprocal increase in a_2. Further increase in water amount leads to an a_2 increase up to ~70%. Based on the spectroscopic data one would be tempted to assign the longer and major component at lower ω_0 to the H-aggregate responsible for absorption ~400 nm. A biexponential decay with lifetimes of 9.20 ns (90%) and of 1.5 ns was reported for TSPP H-aggregate in CTAB/water systems and a lifetime value of 9.26 ns for the monomer in solution given.

Protein–TSPP in AOT reverse micelles

$pH_{ext} = 7$: Protein (HSA or βLG) addition to a solution containing TSPP in AOT RM at a fixed value of ω_0 ($\omega_0 = 15$) causes a bathochromic effect in the absorption Soret band with a maximum at 408 nm and the appearance of a shoulder around 420 nm that becomes the new band maximum at high protein concentrations, Figure 4A, similar to the spectra obtained for TSPP–HSA complex in water.[16b] No isosbestic points were found upon protein addition. By contrast, in fluorescence spectra two isoemissive points were detected, Figure 4B, which enable the assignment of two species in equilibrium. A blue-shift in the first vibronic band occurs accompanied by an increase in intensity and spectral narrowing that suggest a deaggregation process induced by the presence of the protein, although somewhat weaker ($K_b \approx 0.5 \pm 0.2 \times 10^6\ M^{-1}$) than in free aqueous solution.

$pH_{ext} = 2$: We tested for the presence of protein in solutions of TSPP/RM at two extreme water contents, $\omega_0 = 5$ and 30 (see Figure 5). Since in AOT RM both aggregation types are promoted a priori by the encapsulation, the protein effect is less notorious than in aqueous solution. At the lower water concentration, the absorbance of the Soret band (together with a 3 nm red-shift) and of that concerning J-aggregates increased (Figure 5A). Upon excitation at 400 nm, TSPP fluorescence increases greatly with no apparent shift (max ~657 and 721 nm) but with a slight spectral narrowing, Figure 5B. The presence of protein promotes J-aggregation at the expense of H-aggregates.

At $\omega_0 = 30$, J-aggregation already prevailed in the absence of the protein and increased with the protein addition up to

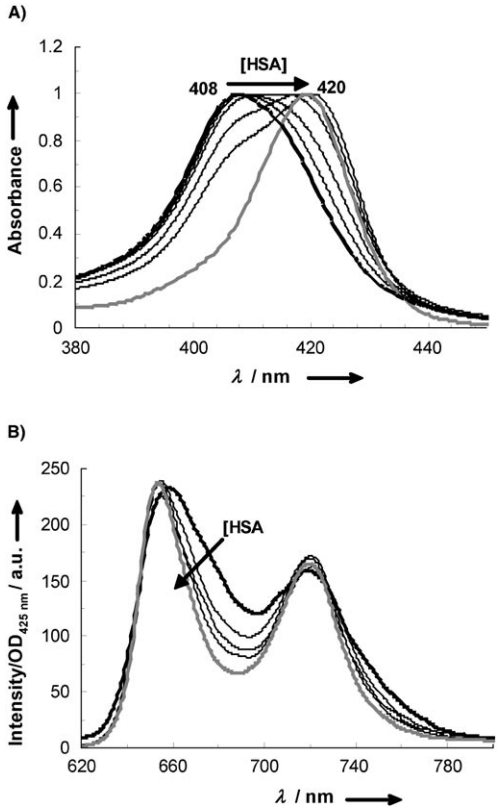

Figure 4. Protein effect on the A) absorption and B) fluorescence of TSPP in AOT RM at $\omega_0 = 15$ and pH 7 ([TSPP] = 1 μM; [HSA] = 0 (black bold), [HSA] = 4.5 μM (grey); $\lambda_{exc} = 425$ nm).

0.05 μM, Figure 5C. Further addition of protein leads to deaggregation as implied by the decrease in the fluorescence intensity ratio collected for the monomer diacid TSPP peak and at the J-aggregate fluorescence peak (Figure 5D). A weaker binding ($K_b \approx 0.1 \pm 0.1 \times 10^6\ M^{-1}$ at $\omega_0 = 5$ and $K_b \approx 1 \pm 1 \times 10^6\ M^{-1}$ at $\omega_0 = 30$) is obtained in AOT RM than in aqueous solution that may arise from changes in the protein conformation;[26] this affects the binding site for TSPP (more important at low ω_0) and/or to competition with aggregation promoted by the AOT RM. The high concentration of electric charges within these RM may also contribute to a weaker binding.

CD data: Similarly to water, in the absence of the protein no CD signal was obtained in the visible region (350–550 nm) for TSPP at $pH_{ext} = 7$ in AOT RM. At $pH_{ext} = 2$ the CD signal intensity depended on ω_0: for $\omega_0 \leq 5$ there was no apparent signal in this spectral region, and we only detected signals for $\omega_0 > 8$ that increased in intensity upon water addition (an exciton couplet centered at 491 nm and another centered at 420.5 nm). Bisignate CD signals obtained both at ~490 and ~420 nm show that both transitions are degenerate. While in the presence of βLG in water (inset Figure 6A) both signals (491 and 420.5 nm) are of comparable intensity, in the case of AOT RM at $\omega_0 = 30$, the signal in the red region is approximately five times greater as com-

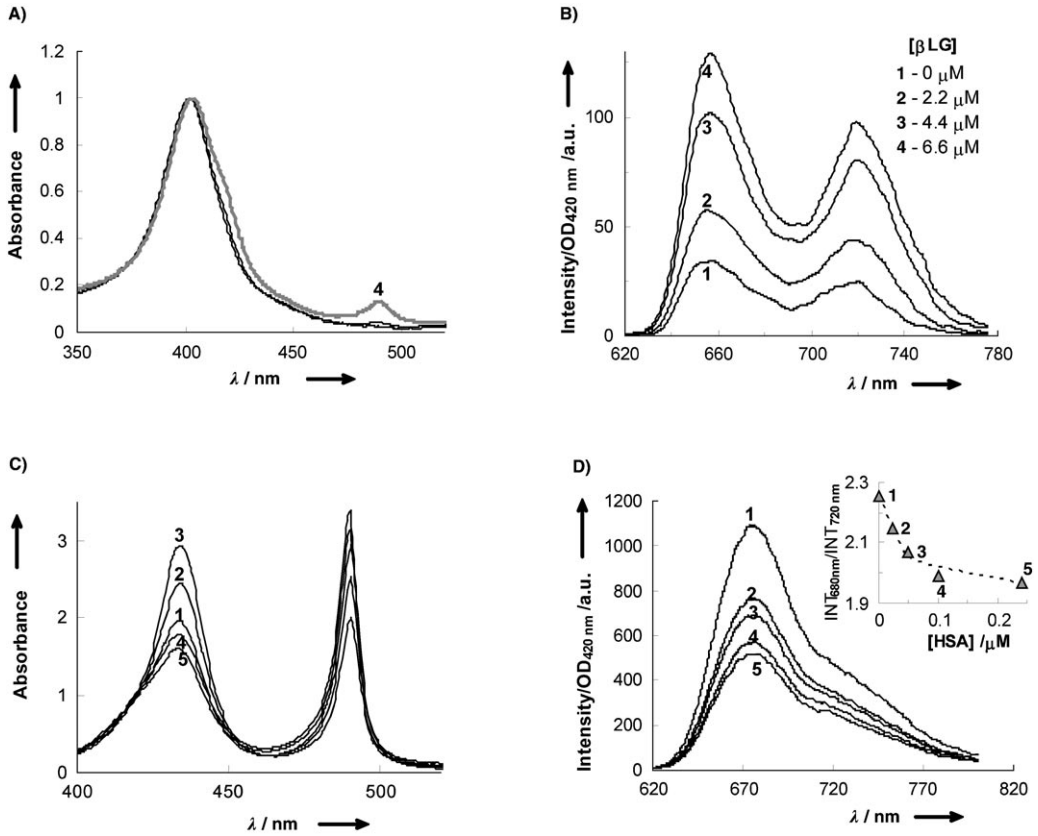

Figure 5. A, C) Absorption and B, D) fluorescence spectra of TSPP in AOT RM in the presence of increasing amounts of protein (A, B) βLG at pH 2 and $\omega_0=5$; (C, D) [HSA] = 0.01–0.24 μM at pH 2 and $\omega_0=30$ ($\lambda_{exc}=420$ nm, [TSPP] ~ 2 μM). Inset: Figure 5D: Dependence of the fluorescence intensity ratio in the monomer/aggregate maxima of TSPP on protein concentration.

pared to that in the blue spectral region. This could mean that different chiral environments are provided by AOT RM and proteins or that the J-aggregate arrangement induced by both systems is geometrically distinct. The order of the bands, namely positive at long wavelength and negative at short wavelength, is indicative of a right-handed orientation of the adjacent units.

Similar experiments were performed at $\omega_0=30$ in the presence of increasing amounts of protein (HSA or βLG), Figure 6B. The signal was more intense for βLG compared with HSA and it increased until [βLG] = 0.2 μM (or until [HSA] = 0.1 μM) above which a steep decrease occurs in the presence of βLG whereas for HSA a smooth one was detected. We also saw differences between each protein in the blue region (positive band at 428 nm and negative band at 417 nm): the signal followed a similar pattern to that in the red region in the case of βLG while a concomitant increase was always observed for HSA. Moreover, in an aqueous solution of free-base TSPP (pH 7) containing HSA, no signal was detected in the 490 nm region, as expected, but a weak signal (= −1 mdeg) was induced at ~420 nm that we assigned to TSPP in a chiral binding site of the protein.

TMpyP–protein interaction

The electrostatic nature of these interactions was also investigated by using a free-base porphyrin positively charged in water and in AOT RM.

In water: Absorption and fluorescence spectra of TMpyP in the presence of different concentrations of βLG in water, Figure 7, resulted in considerable changes; this indicates that the environment of TMpyP alters upon protein binding. A systematic red-shift of the Soret absorption band clearly implied binding of the dye. In general, excited states arising from π–π* transitions such as the Soret transition are expected to decrease in energy as the solvent becomes increasingly hydrophobic, as a consequence of the large dipole moment associated with the π–π* excited state. It has been proposed that even in the presence of concentrated inorganic salts, TMpyP exists as a monomer due to delocalization of the positive charges at the periphery onto the porphyrin ring resulting in electrostatic repulsive forces.[27]

Figure 7B shows that the fluorescence spectrum of TMpyP in water changed from a nonstructured emission band (λ_{max} ~ 720 nm) to two vibrational resolved emission bands (λ_{max} ~ 660 and ~ 720 nm) on increasing the βLG concentration in a similar manner to those obtained in nonprot-

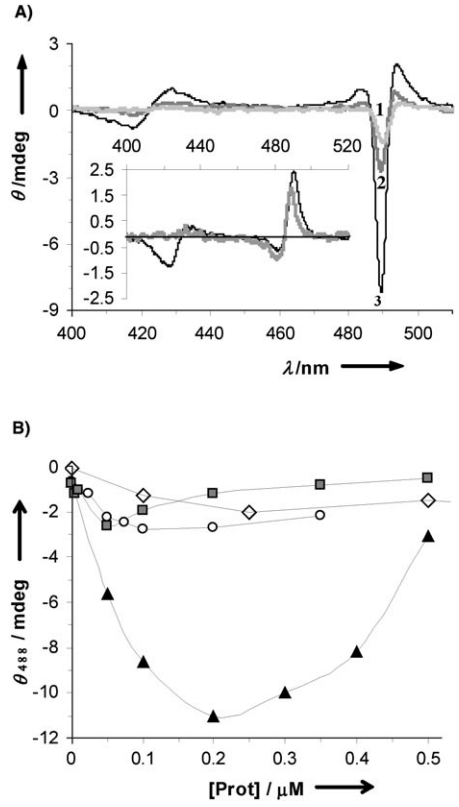

Figure 6. A) Induced CD spectra of TSPP 1) in the absence of protein and in the presence of 2) HSA 0.1 μM; and 3) βLG 0.1 μM, in AOT RM ("pH_{ext}" = 2 and ω_0 = 30) in the absorption region of the complex and J-aggregate. Inset: CD spectra of TSPP in aqueous solution (pH 2) containing 0.1 μM βLG (black line) and 0.05 μM HSA (grey line). B) Dependence of the TSPP CD signal at 486 nm on protein concentration (■) HSA/water; (○) HSA/AOT; (◇) βLG/water; (▲) βLG/AOT RM. [TSPP] = 2 μM.

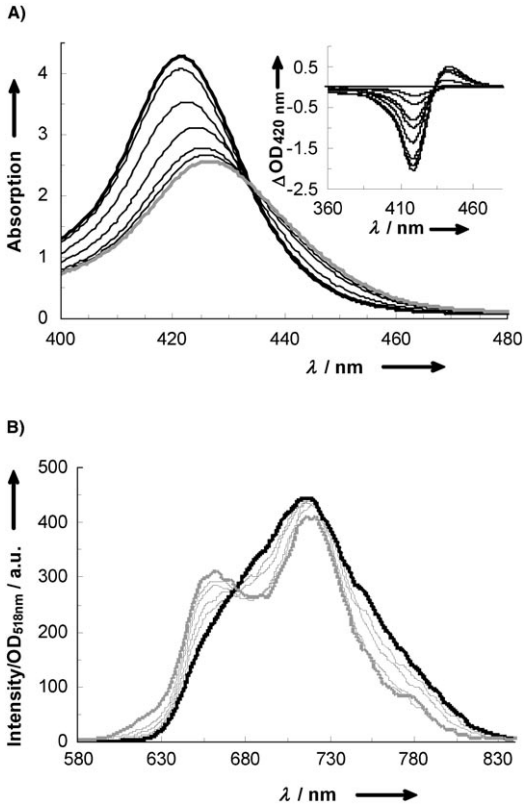

Figure 7. A) Absorption and B) fluorescence emission spectra of TMpyP (2 μM) in aqueous solution (pH 6) in the presence of increasing concentrations of βLG = 0 (black bold); βLG = 20 μM (grey bold); exc = 518 nm; optical density values are multiplied by 10.

ic or apolar solvents.[27,28] These bands are consistent with π–π complex formation between βLG local residues and the porphyrin since complexation is expected to exclude water molecules from the solvation shell of the porphyrin, thus resulting in effective dielectric changes, similar to those reported for interaction with CT-DNA and DNA nucleotides.[29]

Fluorescence decay of TMpyP in water could only be fitted to biexponential functions. We detected a third component upon addition of βLG that increases in weight at the expense of the other two components and seems to confirm the presence of a TMpyP–βLG complex. The origin of the other two components is controversial according to the literature concerning the possibility of TMpyP aggregation.[30] Recent data related these two components with the high affinity of this porphyrin for surfaces.[27] In the presence of methanol, surfactants, or upon increase of temperature, or dilution of aqueous solutions below 10^{-7} M, the single almost structureless fluorescence band resolves into the usual two well-resolved vibrational bands. These changes were attributed to an intramolecular mechanism involving mixing between the S_1 excited state and a nearby higher CT state,[27] the amount of mixing being greatly influenced by solvent polarity thus disproving the TMpyP self-aggregation hypothesis.

From both absorption and fluorescence data, a binding constant $K \sim (2.30 \pm 0.05) \times 10^4$ can be deduced from Equation (1):

$$[\text{porphyrin}]_b = [\text{porphyrin}]_{max} \frac{(K[\text{porphyrin}]_f)^n}{1 + (K[\text{porphyrin}]_f)^n} \qquad (1)$$

where b and f refer to the bound and free porphyrin, K is the equilibrium binding constant, and if there is cooperativity in the binding process n expresses the system heterogeneity, (n varied between 0.89 ± 20; for $n = 1$ we apply the usual Scatchard's equation). The binding constant for the cationic porphyrin is weaker than for the anionic one ($K \sim 3 \times 10^6$) and is independent of pH. While the total charge of TMpyP is 4+ at all pH values tested, the TSPP macrocycle ring deprotonates at pH ~ 4.8 (changing the TSPP global charge from 2− at pH 2.0 to 4− at pH 7.0, see Scheme 1). The binding depends on the conformational structure of the sites and their accessibility that in turn may be affected by the protonation of local residues (like aspartate and glutamate). TMpyP binding seems to be unaffected by these conformational changes that on the one hand suggests that TMpyP is located on an external binding site such as TSPP but on the other points to a more important role of hydrophobic inter-

actions in the case of TMpyP while electrostatic interactions dominate for TSPP.

Binding of substrates to proteins can often cause quenching of the intrinsic Trp fluorescence.[16b,31] Addition of TMpyP (2–10 μM) to βLG in water resulted in saturable, concentration-dependent quenching of the Trp fluorescence and an increase in the TMpyP fluorescence at 715 nm. We were able to estimate the intrinsic dissociation constant for binding, K_d and the maximum quenching reached at saturation, ΔF_{max}, by fitting the quenching data to Equation (2) representing different binding sites with some degree of interaction, where n is the Hill coefficient (the measure of cooperativity of the interaction).[32]

$$\frac{\Delta F}{F_0} = \frac{(\Delta F_{max}/F_0)[\text{porphyrin}]^n}{K_d + [\text{porphyrin}]^n} \quad (2)$$

The errors and statistical significance were determined as described elsewhere.[16b] The value of $K_d \sim 40$ μM ($K \sim 2.5 \times 10^4$) for a $\Delta F_{max} \sim 103\,\%$, inset Figure 8, is similar to that obtained using the absorption or fluorescence of TMpyP in the presence of βLG. Thus, Trp residues within βLG are sensitive to TMpyP binding and, in contrast to TSPP binding at pH 2, quenching data quantitatively suggests such binding affinity is probably due to the fact that some TSPP is aggregated while aggregation does not seem to occur with TMpyP. Fluorescence lifetime measurements were also performed confirming the existence of both static and dynamic quenching.

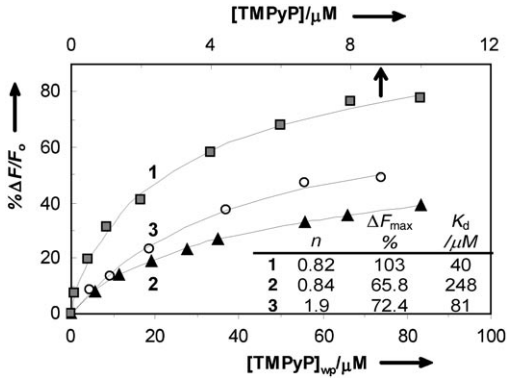

Figure 8. Effect of TMpyP binding on Trp intrinsic fluorescence of βLG ($\lambda_{exc} = 295$ nm, $\lambda_{em} = 338$ nm) in different systems, pH 6: 1) water; 2) AOT ($\omega_0 = 5$); 3) AOT ($\omega_0 = 30$). Parameters (see inset) were obtained by using Equation (2) from the text, where analytical concentrations were used in water whilst local concentrations were used in RM.

In AOT microemulsions: TMpyP exhibits vibrational well-resolved fluorescence spectra in AOT microemulsions at different ω_0. Comparing TMpyP fluorescence in pure solvents[27] one may infer that TMpyP partitions between the interface and the water-pool showing evidence of only a small increase in intensity upon ω_0 increase. Addition of βLG induces a decrease in the intensity ratio I_{blue}/I_{red} of the other two bands that can be related to the porphyrin being located in a less-polar environment.

Fluorescence quenching of Trp was also detected at both $\omega_0 = 5$ and $\omega_0 = 30$ after addition of TMpyP. By using Equation (2) once again it was possible to obtain the dissociation constant and ΔF_{max} under those conditions. The quenching process is, thus, more efficient at $\omega_0 = 30$ although less than for that in pure water, but the binding seems to be stronger at this ω_0. The cooperativity of the process differs at $\omega_0 = 30$ ($n = 1.9$) in comparison to $\omega_0 = 5$ or water ($n \sim 0.83$) that could be linked to changes in the nature of prevailing electrostatic/hydrophobic interactions.

Quenching could arise by a direct interaction (static) or by FRET, due to the extensive overlap between the porphyrin absorption and Trp emission spectra. However, FRET leads to shorter Trp lifetime residues. Fluorescence lifetime measurements of βLG in the presence of TMpyP showed only a minor decrease in both τ_F at the two studied ω_0. At first, these results suggest that quenching by TMpyP may take place by a direct static binding mechanism. However, given the significant quenching obtained, it seems more reasonable to propose that direct binding is only possible for one of the Trp residues and that the other Trp is close enough to TMpyP that effective energy transfer may occur. Thus, this residue would be completely quenched by FRET while the other would contribute to the fluorescence with an almost unchanged lifetime. The R_0 value calculated[25] for the Trp–TMpyP complex was 40 Å and a ≈20 Å center-to-center distance and does not allow us to select a certain preferential binding site for TMpyP on βLG. Nevertheless, the R_0 value is comparable to that in free water and seems to confirm an heterogeneity in binding with possible interchange among binding sites.

Discussion

TSPP H- and J-type aggregation in RM: These results suggest the existence of different aggregates of TSPP in AOT reverse micelles which depend on the amount of solubilized water and local pH. As mentioned before[18c,22c,33] the water in these RM has peculiar solvent properties which are quite different from those of free water (higher viscosity, lower dielectric constant) and therefore the water activity must be such that the usual concept of pH is no longer valid. Moreover, the size of the water-pools (or even the shape for some RM)[18c,34] depends on ω_0. The charge of the surfactant headgroup and the lipophylic balance between the headgroup and the alkyl chain also condition the local environment and contribute to geometrical constraints.

At very low water concentration ($\omega_0 = 3$–4) there are two TSPP species that are independent of pH_{ext}: a monomer in a more hydrophobic environment and an aggregated porphyrin. Spectral deconvolution using Gaussian curves indicates the presence of monomers absorbing at ~419 nm, in a similar way to TSPP in solvents such as DMSO. The aggregated species clearly prevail, probably as dimers due to micellar size constraints, and are responsible for the large blue-shift-

ed Soret band (~402 nm). According to molecular exciton theory, in the H-type configuration the dipolar coupling between monomers leads to the transition where the higher energy becomes allowed and hence absorption is hypsochromically shifted. If electronic states interact with vibronic states, radiative decay from the lower forbidden state will be possible leading to weak emission with a broad red-shifted band. This agrees well with fluorescence data at low ω_0, that essentially show the contribution from the monomer in a less-hydrophilic environment, due to the low fluorescence quantum yield and spectral similarity shown by the H-aggregates (emitting more to the red ~680 nm). This picture is supported by fluorescence decay rates dominated by the long component $\tau_f \approx 12.5$ ns (=75% at $\omega_0 = 8$) that may be assigned to the micellized monomer that is also dominant in aprotic solvents such as DMSO or acetonitrile.[16b]

On the basis of spectral evidence it was stated that the dianionic TSPP could form both J- and H-aggregates by just increasing the porphyrin concentration (above 5×10^{-5} and 10^{-4} M, respectively).[7a] On the other hand, an H-aggregate structure is clearly not favored in ionized-TSPP forms due to Coulombic repulsion between the positive macrocycle or the negative sulfonate groups. However, H-type association would be more facilitated in the case of the tetranionic TSPP due to the absence of charges in the macrocycle and if there were free positive charges capable of spacing and shielding the repulsion between sulfonate adjacent groups. Therefore, the presence of Na^+ counterions in AOT RM, in great excess relative to the porphyrin, could contribute to H-aggregate formation, similar to what is observed for the interaction of TSPP with polylysine,[35] dendrimers, potassium ions, and crown ethers. In the micellar systems, as well as in dendrimers, it is reasonable to assume a relatively even distribution of charge in a spherical geometry. So, aggregation could occur near the charged headgroups (or terminal-charged groups in PAMAM dendrimers) with the porphyrin plane in the H-aggregate in a nearly orthogonal position to the micelle surface probably assuming a "picket-fence" geometry. In the AOT RM at low ω_0, TSPP cannot solubilize in the continuous organic phase nor is there a well defined water-pool. The existing water, mainly hydrating the headgroups at least up to $\omega_0 = 6$, and the Na^+ counterions do not have high mobility. An ordered aggregation is then facilitated by the presence of such less-mobile positive charges and the hydrophobic clustering of the medium. Increasing the amount of water gives another solubilization site for TSPP and the concentration in H^+ also shifts the pK_a to higher values (close to that in free aqueous solution). This is reflected by the dissociation of H-aggregates to form different arrangements, J-aggregates ("deck-of-cards" spread and/or zig-zag, corresponding to a head-to-tail alignment of transition dipole moments),[36] and monomers, at pH 2, or essentially monomers at pH 7, that are also facilitated by the increase in the hydrodynamic radius of the RM and the decrease in the number of micelles. In fact, on increasing the number of micelles we detect a clear pattern of aggregate dissociation and monomers are obtained.

The exciton theory allows for a calculation of the spectroscopic aggregation number N, from the spectral width of the absorption band of the J-aggregate, this being proportional to $N^{-1/2}$. We observe a spectral narrowing of the J-aggregate absorption band with increasing ω_0. A spectral deconvolution of the Soret band by using a sum of Gaussian curves enables the identification of the absorption band of the monomeric species ($\lambda_{max} = 434$ nm) that is detected only for $\omega_0 \geq 20$. The value of the fwhm obtained (866 cm^{-1}) is very similar to the monomer in acidic aqueous solution (875 cm^{-1}). Calculations indicate an increase of the aggregation number ($N = 6.4$–10.7 molecules at $20 \leq \omega_0 \leq 50$) with the water-pool radius increase (Figure 9).

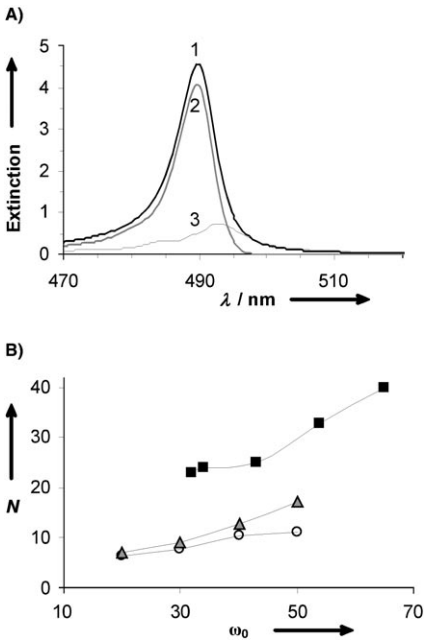

Figure 9. A) Extinction spectrum of 1) TSPP ([TSPP] = 2 μM) in the J-band region, in AOT RM ($\omega_0 = 40$, "pH_{ext}" = 2) and the contributions from the 2) absorption and 3) scattering components. B) Spectroscopic aggregation number (N) dependence on the amount of water in the system: without scattering correction (○); and with scattering correction (▲); (■). The latter were taken from ref. [15b].

Recent reports showed that the spectra obtained from the spectrophotometer "extinction spectra" are subject to appreciative scattering and are therefore, different from the "true spectra". These can be corrected by removing the scattering contribution given by the RLS spectra.[15b,37,38] Hence, the "corrected" values of N lie in the range of 7.1–17.4. These are lower than those reported for TSPP in AOT/decane/water RM[15b] where N values are of the order of 23–33. Due to the longer alkyl chain of the organic solvent (decane) one would expect that larger RM could be formed and the percolation phenomena would be important for the higher ω_0 at room temperature allowing a further growth of the aggregates. But, hydrodynamic radii reported are equivalent to those obtained when the organic phase is isooctane. On the other hand, that investigation used a citrate buffer with a similar concentration to the one we used but our

buffer also contained phosphate. Also, the porphyrin concentrations used in that study are approximately 20 times higher which could justify the differences obtained in the N values. A comparable value is reported for TSPP (10 μM, pH 3.0) J-aggregates in the presence of high salt concentrations (NH_4Cl ~0.1 M), $N=12.9$ that showed also that the coherence length was about 25% of the aggregate hydrodynamic radius.[37a] Although exciton theory is generally accepted to explain spectral shifts and narrowing of bands due to J-aggregates, N values are calculated assuming only the motional/exchange narrowing mechanism. If we consider other effects (temperature and static/dynamic disorder) we could obtain a closer coherence value and physical size of the aggregate. In AOT/decane/water RM values of 100 and 35% for $\omega_0=32$ and $\omega_0=65$, respectively, were obtained pointing to a high exciton delocalization very close to an ideal J-aggregate structure.

There is some controversy in the literature concerning the origin of the 420 nm band and TSPP aggregation. The band has been assigned to an H-aggregate of TSPP based on Raman data.[6c] The synchronous variation of the CD signal and the intensity of both the 490 and 420 nm band led others to attribute both bands to the J-aggregate.[6a] The calculated value for the blue-shift of the B-band (taking into account the face-to-face packing in the H-aggregate) is much larger than the experimental one at 420 nm. Thus, it seemed more plausible to attribute bands 490 and 420 nm to the splitting of the TSPP B-band as a consequence of the lowering of the symmetry of the porphyrin macrocycle in the aggregates.[39] On the other hand, based on the fact that these colloidal structures are CD-active due to the spontaneous symmetry break-down as shown in Figure 6, it was possible to infer the presence of two exciton orthogonal chirality axes corresponding to the J- and H-aggregation in the supramolecular structure due to the folding of the one-dimensional aggregates.[40] A comparison of our data (absorption and CD spectra) of TSPP in acidic conditions in AOT ($\omega_0=50$) and in an aqueous solution of HSA, clearly shows that with TSPP/AOT only two Q-bands are detected (besides those corresponding to J-aggregates) while for TSPP/HSA four Q-bands are observed with maxima similar to those detected in DMSO. The Soret band maximum is at ~420 nm in both cases. In conclusion, the spectroscopic species of TSPP responsible for the ~420 nm maximum obtained in the presence of HSA cannot be the same as that obtained in AOT $\omega_0\geq 10$. The spectroscopic aggregation number (N) calculated from the spectral width of the absorption band of the J-aggregate is very different for TSPP in the presence of protein (N~6–7 units) to that calculated for AOT reverse micelle systems (7–17 units). Moreover, we did not detect J-aggregates at pH 7 but the B-band due to monomer shifted to 420 nm and gave a low-intensity CD signal in that region (=−1 mdeg), as mentioned before. In addition, the full-width-at-half-height of the 420 nm absorption band is ~850 cm^{-1} in the case of TSPP/HSA at both pH 2 or 7, while a much broader band is obtained from spectral deconvolution for TSPP/AOT ($\omega_0=30$).

Comparison with other micellar systems: To test the importance of the surfactant headgroup charge we performed experiments involving other RM formed with the cationic TTAB and the neutral Triton X-100 surfactant. We observed no significant spectral changes (see data in Table 1) in the neutral system apart from a small blue-shift as the water amount was increased reflecting the environment polarity/polarizability. In the cationic system, TSPP is mainly at the interface as a monomer that may diffuse to the hydrophilic interfacial region at high water concentrations where a small contribution of the diacid species is noted together with some J-type aggregation. Therefore, TSPP shows a major tendency to aggregate in anionic RM systems. A schematic view of the aggregation pattern in these AOT RM is given in Scheme 2. By contrast, in the aqueous micellar system we

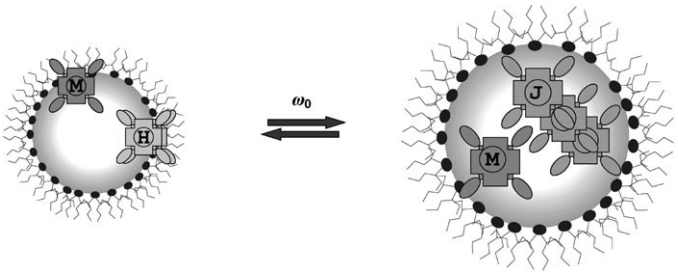

Scheme 2. Schematic diagram representing the influence of water uptake on the TSPP aggregation pattern and location inside AOT RM in the absence of protein.

only observed aggregation with the cationic species. Nevertheless, electrostatic interactions may not be the exclusive driving-force for the process since shorter-chain surfactants are only able to induce aggregation at higher concentrations.[13]

Comparison with a positively charged porphyrin, TMpyP: TMpyP does not seem to aggregate either in the presence of the protein in water or in AOT RM. By contrast, for a metal-derivative Pd^{II}TMpyP in AOT RM, when there are only a few water molecules available for adsorption at the interface ($\omega_0=0.13$) porphyrin molecules may strongly interact with the surfactant headgroups leading to ion-pair formation, and this has also been confirmed in the case of Zn^{II}TMpyP.[24c] Similar steady-state absorption spectra were obtained for TMpyP, but only in aqueous AOT at pre-micellar surfactant concentrations. The aggregation is facilitated by either Coulombic attraction between the ionic surfactant and the oppositely charged aromatic molecule, and by the hydrophobic clustering of the surfactant alkyl chains. Curiously, this aggregate is spectroscopically different from that reported[13] in SDS pre-micellar concentrations. The effect of protonation of the pyrrole nitrogen atoms on the aggregation condition of TMpyP cannot be followed in the RM system since that would require the use of HCl (1 M, pK_a~0.9) and produce an unstable system.

Another important difference between the two porphyrins in the presence of proteins is the observed fluorescence quenching of TMpyP by βLG, that occurred both in water

and in AOT RM. A Stern–Volmer plot of the fluorescence intensity ratio of TMpyP in the absence and presence of quencher as a function of the quencher concentration ([βLG]), does not show a linear dependence but a downward curvature. Moreover, the quenching rate constant is higher in water than in AOT RM ($\omega_0=30$) while no apparent quenching could be detected at $\omega_0=5$. The process may involve electron transfer from certain residues in the protein (probably lysine and/or arginine residues which have a tertiary amine side chain).

Conclusion

The results described in the present study point to both similarities and differences in the interaction of TSPP and TMpyP porphyrins with drug-carrier proteins in water and in AOT RM.

We detected complex TSPP aggregation that is dependent on change of water-content and pH when the TSPP is encapsulated in AOT RM. We may infer that higher water-contents are more suitable to J-aggregation whereas a decrease in ω_0 leads to aggregate distortion and formation of a wide distribution of aggregates with various structures, namely an H-aggregate for very low ω_0. The presence of protein contributes to H-deaggregation but promotes J-aggregation at least up until a ratio of the relative concentration is reached, above which, complexation competes.

From point dipole exciton theory, the spectral features of Soret bands indicate a growth in the aggregation number of J-aggregates upon increase in the size of the water-pools.

The confinement effect created by the AOT water-pool enables the tuning of photophysical properties of the nanoaggregates formed, and opens up new ways for exploiting them for nonlinear optics.

Coulombic interactions between TMpyP and AOT prevented porphyrin aggregation and led to weaker affinity to the transport protein. A different binding site is possible for TMpyP complexation to the proteins studied which leads to a weak but effective fluorescence quenching of the porphyrin by some amino acid residues in the protein.

Experimental Section

Sample preparation: HSA fraction V, 96–99% purity (catalogue no. A-1653), bovine βLG chromatographically purified and lyophilized ≥90% purity (catalogue no. L-3908), TMpyP (catalog no. T-0644), AOT (catalogue no. D-4422) ≥99% purity, and TTAB (catalogue no. T-4762) 99% purity, were purchased from Sigma (St. Louis, MO) and were used without further purification. TSPP was obtained from Fluka ≥98% purity (catalogue no. 88074). Triton X-100 was purchased from Riedel-de-Häen and purified as mentioned elsewhere.[41] Buffer solutions were made up with bidistilled water, following the recommended procedures. In the pH 2–7 range, a citrate/phosphate buffer (25 mM) was employed. All solvents were spectroscopic grade. In all experiments we used fresh stock solutions of proteins.

A stock solution of AOT/isooctane (0.1 M) was prepared and checked for fluorescence emission that was negligible under the experimental conditions used. Reverse micelle solutions were then prepared by direct addition of bidistilled water into the surfactant/hydrocarbon mixture (volume fraction of dispersed phase $\phi_v=0.1$). The protein was also added by the injection method. All the volume injected was considered to be water and was used to calculate ω_0 ($\omega_0=[H_2O]/[AOT]$). A transparent solution was always obtained after shaking for a few seconds. We used the the Karl–Fischer method to determine the amount of water in the dry micelle solution ($\omega_0=0.15$).[42] The probe concentrations were determined spectrophotometrically considering the molar extinction coefficient $\varepsilon_{280\,nm}^{HSA}=42\,864\,M^{-1}cm^{-1}$;[43] $\varepsilon_{280\,nm}^{\beta LG}=17\,600\,M^{-1}cm^{-1}$ for the protein monomer;[44] $\varepsilon_{413\,nm}^{TSPP}=5.1\times10^5\,M^{-1}cm^{-1}$ at pH 6,[45] and $\varepsilon_{422\,nm}^{TMpyP}=2.26\times10^5\,M^{-1}cm^{-1}$.[46]

Apparatus: A Jasco V-560 spectrophotometer was employed in UV-visible absorption measurements. Fluorescence measurements were recorded with a Perkin–Elmer LS 50B spectrofluorimeter. Band-pass slits of 7.5 nm were used for both fluorescence excitation and emission monitoring of TSPP. The instrumental response at each wavelength was corrected by means of a curve obtained using appropriate fluorescence standards together with the one provided with the instrument. RLS spectra were obtained by using synchronous excitation and emission scanning in a right-angle geometry and were corrected by subtracting the corresponding blank sample. The "true" absorption spectra, $A_{abs}(\lambda)$, were derived from those obtained directly from the spectrophotometer, $A_{em}(\lambda)$, for samples where RLS spectra showed a relevant signal, $I_{RLS}(\lambda)$, by using $A_{em}(\lambda)=A_{abs}(\lambda)+aI_{RLS}(\lambda)+b$.[37b] The empirical parameters a and b, account for the monochromator features, detector and system geometry, and were determined by linear fitting of $A_{em}(\lambda)$ versus $I_{RLS}(\lambda)$ in the (520–560 nm) region where $A_{abs}(\lambda)=0$.

Fluorescence quantum yields of aerated solutions of TSPP and TMpyP were determined relative to that of TPP in toluene ($\phi\approx0.11$)[47] with appropriate corrections for the refractive index of the solvent. Fluorescence decay profiles were obtained by using the time-correlated single-photon counting method[48] with a Photon Technology International (PTI) instrument. Excitation was induced with the use of a lamp filled with H_2 ($\lambda_{exc}^{Porphyrin}=420$ nm) and sample emission measurements ($\lambda_{em}^{Porphyrin}=650$ nm) were performed upto a maximum of 10^4 counts. Data analysis was performed by a deconvolution method using a nonlinear least-squares fitting program based on the Marquardt algorithm. The goodness-of-fit was evaluated by statistical parameters (reduced χ^2 and Durbin–Watson (DW)) and graphical methods (autocorrelation function and weighted residuals).

CD spectra were obtained by using a Jasco J-720 spectropolarimeter (Hachioji City, Tokyo). An average of 4–8 scans was recorded and corrected by subtracting the baseline spectrum of unfilled RM with the same composition as the sample. The studies were performed at a constant porphyrin concentration (2 μM) in the visible range and water or protein concentration was varied. We used 1 cm path-length quartz cells and the temperature was maintained at 24.0±0.5 °C.

Acknowledgements

This work was supported by Project POCTI/35398/QUI/2000. The authors thank Professor J. Costa Pessoa for the use of a CD spectrometer. S.M.A. thanks the FCT for a BPD grant 9439/2002.

[1] a) R. Bonnett, *Chem. Soc. Rev.* **1995**, *24*, 19–33; b) I. J. MacDonald, T. J. Dougherty, *J. Porphyrins Phthalocyanines* **2001**, *5*, 105–129; c) D. Kessel, P. Thompson, K. Saaito, K. D. Nantwi, *Photochem. Photobiol.* **1987**, *45*, 787–790.

[2] G. Labat, J. L. Séris, B. Meunier, *Angew. Chem.* **1990**, *102*, 1488–1490; *Angew. Chem. Int. Ed. Engl.* **1990**, *29*, 1471–1473.

[3] T. Tsuchida, G. Zheng, R. K. Pandey, W. R. Potter, D. A. Bellinier, *Photochem. Photobiol.* **1997**, *66*, 224–228.

[4] J. P. Keene, D. Kessel, E. J. Land, R. W. Redmond, T. G. Truscott, *Photochem. Photobiol.* **1986**, *43*, 117–120.

[5] a) P. W. Bohn, *Ann. Rev. Phys. Chem.* **1993**, *44*, 37–60; b) E. W. Knapp, *Chem. Phys.* **1984**, *85*, 73–82; c) W. I. White in *The Porphyrins, Vol. V*, (Ed.: D. Dolphin), Academic Press, New York, **1979**.
[6] a) O. Ohno, Y. Kaizu, H. Kobayashi, *J. Chem. Phys.* **1993**, *99*, 4128–4139; b) N. C. Maiti, M. Ravikanth, S. Mazumdar, N. Periasamy, *J. Phys. Chem.* **1995**, *99*, 17192–17197; c) D. L. Akins, H.-R. Zhu, C. Guo, *J. Phys. Chem.* **1994**, *98*, 3612–3618.
[7] a) J. M. Ribó, J. Crusats, J.-A. Farrera, M. L. Valero, *J. Chem. Soc. Chem. Commun.* **1994**, 681–682; b) R. Rubires, J. Crusats, Z. El-Hachemi, T. Jaramillo, M. López, E. Valls, J.-A. Farrera, J. M. Ribó, *New J. Chem.* **1999**, 189–198.
[8] S. C. M. Gandini, E. L. Gelamo, R. Itri, M. Tabak, *Biophys. J.* **2003**, *85*, 1259–1268.
[9] F. Mallamace, N. Micali, S. Trusso, L. M. Scolaro, A. Romeo, A. Terracina, R. F. Pasternack, *Phys. Rev. Lett.* **1996**, *76*, 4741–4744.
[10] P. J. Collings, E. J. Gibbs, T. E. Starr, O. Vafek, C. Yee, L. A. Pomerance, R. F. Pasternack, *J. Phys. Chem. B* **1999**, *103*, 8474–8481.
[11] N. Micali, F. Mallamace, A. Romeo, R. Purrello, L. M. Scolaro, *J. Phys. Chem. B* **2000**, *104*, 5897–5904.
[12] R. Rotomskis, R. Augulis, V. Snitka, R. Valiokas, B. Liedberg, *J. Phys. Chem. B* **2004**, *108*, 2833–2838.
[13] N. C. Maiti, S. Mazumdar, N. Periasamy, *J. Phys. Chem. B* **1998**, *102*, 1528–1538.
[14] a) F. Mallamace, L. M. Scolaro, A. Romeo, N. Micali, *Phys. Rev. Lett.* **1999**, *82*, 3480–3483; b) S. M. Andrade, S. M. B. Costa, *J. Fluoresc.* **2002**, *12*, 77–82.
[15] a) S. C. M. Gandini, V. E. Yushmanov, I. E. Borissevitch, M. Tabak, *Langmuir* **1999**, *15*, 6233–6243; b) M. A. Castriciano, A. Romeo, V. Villari, N. Micali, L. M. Scolaro, *J. Phys. Chem. B* **2004**, *108*, 9054–9059.
[16] a) I. E. Borissevitch, T. T. Tominaga, H. Imasato, M. Tabak, *J. Lumin.* **1996**, *69*, 65–76; b) S. M. Andrade, S. M. B. Costa, *Biophys. J.* **2002**, *82*, 1607–1619.
[17] a) P. M. R. Paulo, S. M. B. Costa, *Photochem. Photobiol. Sci.* **2003**, *2*, 597–604; b) P. M. R. Paulo, R. Gronheid, F. C. De Schryver, S. M. B. Costa, *Macromolecules* **2003**, *36*, 9135–9144.
[18] a) P. L. Luisi, M. Giomini, M. P. Pileni, B. H. Robinson, *Biochim. Biophys. Acta* **1988**, *947*, 209–246; b) S. M. Andrade, S. M. B. Costa, R. Pansu, *Photochem. Photobiol.* **2000**, *71*, 405–412; c) S. M. Andrade, S. M. B. Costa, R. Pansu, *J. Colloid Interface Sci.* **2000**, *226*, 260–268.
[19] a) M. Zulauf, H.-F. Eicke, *J. Phys. Chem.* **1979**, *83*, 480–486; b) G. Cassini, J. P. Badiali, M. P. Pileni, *J. Phys. Chem.* **1995**, *99*, 12941–12946.
[20] a) H. Kunieda, K. Shinoda, *J. Colloid Interface Sci.* **1979**, *70*, 577–583; b) W. Meier, H.-F. Eicke, *Curr. Opin. Colloid Interface Sci.* **1996**, *1*, 279–286.
[21] P. Walde, Q. Peng, N. W. Fadnauis, E. Battistel, P. L. Luisi, *Eur. J. Biochem.* **1988**, *173*, 401–410.
[22] a) D. Christopher, J. Yarwood, P. S. Belton, B. P. Hills, *J. Colloid Interface Sci.* **1992**, *152*, 465–471; b) H. Christenson, S. E. Friberg, D. W. Larsen, *J. Phys. Chem.* **1980**, *84*, 3633–3638; c) M. D′Angelo, G. Onori, A. Santucci, *Riv. Nuovo Cimento Soc. Ital. Fis.* **1994**, *16*, 1601–1611.
[23] J. Faeder, B. M. Ladanyi, *J. Phys. Chem. B* **2000**, *104*, 1033–1046.
[24] a) D. M. Togashi, S. M. B. Costa, *Phys. Chem. Chem. Phys.* **2000**, *2*, 5437–5444; b) A. S. Tatikolov, S. M. B. Costa, *Photochem. Photobiol. Sci.* **2002**, *1*, 1–9; c) M. Aoudia, M. A. J. Rodgers, *J. Phys. Chem. B* **2003**, *107*, 6194–6207; d) D. M. Togashi, S. M. B. Costa, A. J. F. N. Sobral, A. M. d′A. R. Gonsalves, *J. Phys. Chem. B* **2004**, *108*, 11344–11356.
[25] $R_0 = 0.2108(k^2\phi_f^0 n^{-4} \int F(\lambda)\varepsilon(\lambda)\lambda^4 d\lambda)^{1/6}$ where k^2 is the orientation factor ($^2/_3$ assumed) describing the relative orientation in space of the transition dipoles of the donor (Trp residues) and acceptor (porphyrin), ϕ_f^0 is the donor quantum yield in the absence of the acceptor, n is the refractive index of the solution, $F(\lambda)$ is the donor normalized fluorescence spectrum, $\varepsilon(\lambda)$ is the acceptor molar extinction coefficient ($M^{-1}\,cm^{-1}$) and λ is in nm; see for example: J. R. Lakowicz, *Principles of Fluorescence Spectroscopy*, Plenum Press, New York, **1983**.
[26] S. M. Andrade, T. I. Carvalho, M. I. Viseu, S. M. B. Costa, *Eur. J. Biochem.* **2004**, *271*, 734–744.
[27] F. J. Vergeldt, R. B. M. Koehorst, A. Hoek, T. J. Schaafsma, *J. Phys. Chem.* **1995**, *99*, 4397–4405.
[28] K. Lang, P. Kubát, P. Lhoták, J. Mosinger, D. M. Wagnerová, *Photochem. Photobiol.* **2001**, *74*, 558–565.
[29] R. Jasuja, D. M. Jameson, C. K. Nishijo, R. W. Larsen, *J. Phys. Chem. B* **1997**, *101*, 1444–1450.
[30] a) R. F. Pasternack, P. R. Huber, P. Boyd, G. Engasser, L. Francesconi, E. Gibbs, P. Fasella, G. C. Venturo, L. Hinds, *J. Am. Chem. Soc.* **1972**, *94*, 4511–4517; b) K. Kemnitz, T. Sakaguchi, *Chem. Phys. Lett.* **1992**, *196*, 497–503.
[31] a) T. K. Das, S. Mazumdar, *J. Phys. Chem.* **1995**, *99*, 13283–13290; b) R. Liu, A. Siemiarczuk, F. J. Sharom, *Biochemistry* **2000**, *39*, 14927–14938.
[32] S. W. Nelson, C. V. Iancu, J.-Y. Choe, R. B. Honzatko, H. J. Fromm, *Biochemistry* **2000**, *39*, 11100–11106.
[33] a) M. Hasegawa, T. Sugimura, Y. Suzaki, Y. Shindo, *J. Phys. Chem.* **1994**, *98*, 2120–2124; b) M. Belletete, G. Durocher, *J. Colloid Interface Sci.* **1990**, *134*, 289–293.
[34] D. Pant, N. E. Levinger, *Langmuir* **2000**, *16*, 10123–10130.
[35] R. Purrello, E. Bellacchio, S. Gurrieri, R. Lauceri, A. Raudino, L. M. Scolaro, A. M. Santoro, *J. Phys. Chem. B* **1998**, *102*, 8852–8857.
[36] D. L. Atkins, H.-R. Zhu, C. Guo, *J. Phys. Chem.* **1996**, *100*, 5420–5425.
[37] a) A. S. R. Koti, J. Taneja, N. Periasamy, *Chem. Phys. Lett.* **2003**, *375*, 171–176; b) N. Micali, F. Mallamce, M. Castriciano, A. Romeo, L. M. Scolaro, *Anal. Chem.* **2001**, *73*, 4958–4963.
[38] When the light is absorbed by a polarizable particle, a larger oscillation is induced and therefore this particle "emits" the absorbed light. In fact, the RLS signal in the absorbing region of the J-aggregate is intense and shows a red-shift (~3 nm) comparatively to the extinction signal. By following the procedure described by others, see ref. [37], we see that the scattering component is rather important in that region leading to a narrower spectrum band but does not really affect the monomer region.
[39] D.-M. Chen, T. He, D.-F. Cong, Y.-H. Zhang, F.-C. Liu, *J. Phys. Chem. A* **2001**, *105*, 3981–3988.
[40] a) J. M. Ribó, J. M. Bofill, J. Crusats, R. Rubires, *Chem. Eur. J.* **2001**, *7*, 2733–2737; b) R. Rubires, J.-A. Farrera, J. M. Ribó, *Chem. Eur. J.* **2001**, *7*, 436–446.
[41] C. Kumar, D. Balasubramanian, *J. Colloid Interface Sci.* **1979**, *69*, 271–279.
[42] K. Fischer, *Angew. Chem.* **1935**, *48*, 394–396.
[43] B. P. Esposito, A. Faljoni-Alário, J. F. S. Meneses, H. F. Brito, R. Najjar, *J. Inorg. Biochem.* **1999**, *75*, 55–61.
[44] M. Barteri, M. C. Gaudiano, S. Rotella, G. Benagiano, A. Pala, *Biochim. Biophys. Acta* **2000**, *1479*, 255–264.
[45] C. Z. Huang, Y. F. Li, K. A. Li, S. Y. Tong, *Bull. Chem. Soc. Jpn.* **1998**, *71*, 1791–1797.
[46] T. Uno, K. Hamasaki, M. Tanigawa, S. Shimabayashi, *Inorg. Chem.* **1997**, *36*, 1676–1683.
[47] T. L. C. Figueiredo, R. A. W. Johnstone, A. M. P. Sørensen, D. Burget, P. Jacques, *Photochem. Photobiol.* **1999**, *69*, 517–528.
[48] D. V. O'Connor, D. Phillips, *Time-correlated Single Photon Counting*, Academic Press, New York, **1984**.

Received: January 14, 2005
Revised: June 17, 2005
Published online: October 26, 2005

